

## Structural Studies of a *N*-[*N*-Unsubstituted Pyrrole-3-carbonyl]oxy]benzamide and its Precursor Spiro[isoxazole-4,3'-pyrrole]

by Giovanni Grassi\*<sup>1)</sup> and Massimiliano Cordaro

Dipartimento di Chimica Organica e Biologica, Università, Vill. S. Agata, I-98166 Messina

and Giuseppe Bruno and Francesco Nicolò

Dipartimento di Chimica Inorganica, Chimica Analitica e Chimica Fisica, Università, Vill. S. Agata, I-98166 Messina

---

The structures of 6-methyl-4,8,9-triphenyl-2-oxa-3,7-diazaspiro[4.4]nona-3,6-dien-1-one (**3**) and *N*-[(2-Methyl-4,5-diphenyl-1*H*-pyrrole-3-carbonyl)oxy]benzamide (**4**) were established by X-ray crystal-structure analysis. A significant improvement in the procedure currently available for the synthesis of these compounds is described. *Ab initio* and DFT calculations were carried out on the compound **4** and its precursor **3**, and compared with X-ray results. In particular, to relate structural features to biological properties, the conformational characteristics and rotational barrier of compound **4** were studied.

---

**Introduction.** – Hydroxamic acid derivatives are synthetic targets of interest, not least because of their biological activity, especially as enzyme inhibitors [1] and metal chelators [2].

We recently described the regioselective synthesis of *N*-(pyrrolecarbonyl)oxy amides by sequential oxazol-5(4*H*)-one cycloaddition and nitrile oxide addition starting from (*Z*)-4-(arylmethylidene)isoxazol-5(4*H*)-ones **1** [3] (*Scheme*). These novel amides **4** appear to have promising biological activity; indeed, one of the derivatives (Ar = 3-MeOC<sub>6</sub>H<sub>4</sub>) was selected for further *in vivo* testing on the basis of initial anticancer screening<sup>2)</sup>.

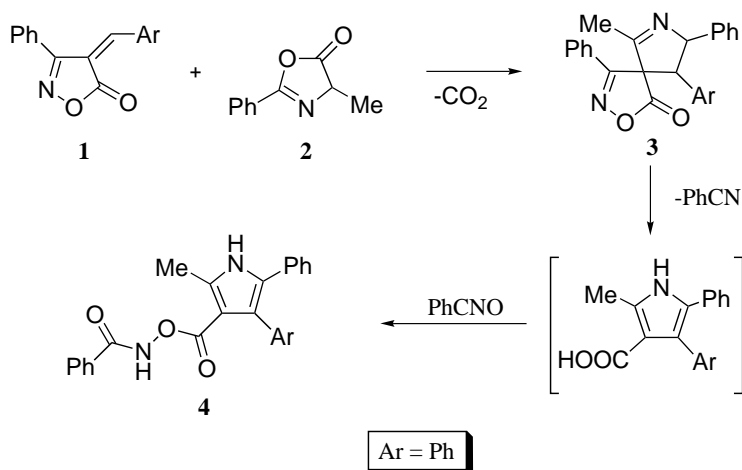
In light of these results, we were encouraged to undertake a study of the molecular structure of compounds **3** and **4** by X-ray crystal-structure analysis. Thus, for the compound **3**, to understand the nature of the geometric distortion due to molecular packing and H-bonds, and to confirm the reliability of the carbonyl bond angle, we describe an *ab initio* geometry optimization. Moreover, since detailed knowledge of the conformational behavior and rotational potential-energy surface is of great importance because various physicochemical and biological properties are strongly influenced by molecular conformations, for compound **4**, we computed the internal rotational barrier around the O–N bond by scanning the corresponding torsional angle with X-ray-structural data as the starting geometry.

---

<sup>1)</sup> Fax: +3990393897, e-mail: ggrassi@isengard.unime.it.

<sup>2)</sup> This study is being carried out at the U.S. National Cancer Institute, Bethesda, Maryland.

Scheme



**Results and Discussion.** – The molecule **3** contains a substituted spiro system obtained by 1,3 dipolar cycloaddition of a mesoionic compound (MPO), 4-methyl-2-phenyloxazol-5(4*H*)-one (**2**), with an 4-(arylmethylidene)isoxazol-5(4*H*)-one (**1**). Crystals are made up of discrete molecules of (8*R*,9*R*)-6-methyl-4,8,9-triphenyl-2-oxa-3,7-diazaspiro[4,4]nona-3,6-dien-1-one separated by normal *Van der Waals* contacts and H-bonds. Besides the spiro atom, the compound has two additional stereogenic centres: C(5) and C(6).

Since the compound crystallizes in the centrosymmetric space group  $P\bar{1}$ , in the solid state, it is a perfect racemic mixture of one of the possible diastereoisomers (*S,S,S*) and (*R,R,R*). *Fig. 1* shows an ORTEP view of an enantiomer with (*S,S,S*) configuration at its stereogenic centres. A molecule of MeOH, used as a crystallization solvent, is present in the asymmetric unit and forms a H-interaction with the atom N(2). The two planes of the spiro center, defined by the atoms C(1)–C(2)–C(3) and C(4)–C(2)–C(6), form an interplanar angle of  $92.6(2)^\circ$ . The least-square plane calculated for the isoxazolone fragment shows how it is perfectly planar and forms a dihedral angle of  $33.53(9)^\circ$  with the Ph plane bonded to C(3) (C(3)–C(7) = 1.470(3) Å). The dihydro pyrrole ring is not flat, and the deviations from the least-squares plane calculated for the five atoms are: C(6) –0.138(2), C(2) 0.106(2), C(4) –0.034(2), C(5) 0.125(2), and N(2) –0.044(2) Å. Puckering parameters [4] ( $Q = 0.221(2)$  and  $\varphi = 140.8(4)^\circ$ ) indicate a distorted envelope conformation. The ring bears as substituents a Me and two Ph groups, which form an interplanar angle of  $98.55(7)^\circ$ . The bond distances and angles involving the spiro atom are in good agreement with corresponding values reported for other spiro[4.4]derivatives [5]: C(2)–C(4) = 1.536(3) Å, C(2)–C(6) = 1.563(3) Å, C(2)–C(3) = 1.502(3) Å, C(1)–C(2)–C(6) =  $113.4(2)^\circ$ , C(3)–C(2)–C(6) =  $114.7(2)^\circ$ , C(3)–C(2)–C(4) =  $118.2(2)^\circ$ , C(1)–C(2)–C(4) =  $110.1(2)^\circ$ , C(3)–C(2)–C(1) =  $100.1(2)^\circ$ , and C(4)–C(2)–C(6) =  $100.9(2)^\circ$ . The difference in bond angles C(3)–C(2)–C(4) and C(1)–C(2)–C(6), which are  $118.2(2)^\circ$  and  $113.3(2)^\circ$ , respectively, are mainly determined by steric hindrance

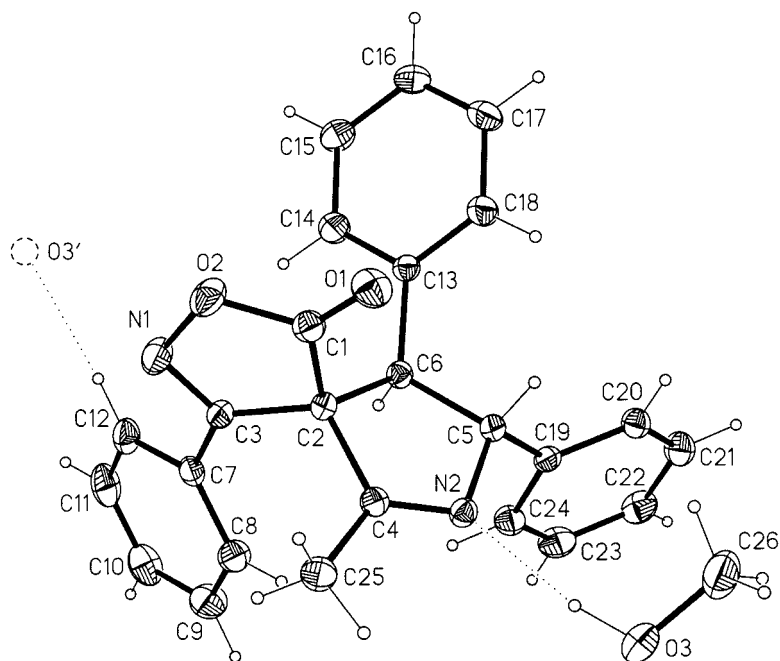


Fig. 1. View of the asymmetric unit of compound **3** with atom numbering scheme and thermal ellipsoids at 40% of probability, while H size is arbitrary. Dotted lines represent the H-interactions  $[\text{C}(x), 1+y, z]$ .

between the Ph group at C(3) and the Me group at C(4) ( $C(8) \cdots C(25) = 3.683 \text{ \AA}$ ). In the isoxazolone fragment, we observe the usual asymmetry in the carbonyl bond angles:  $O(1)-C(1)-O(2) = 121.9(2)^\circ$  and  $O(2)-C(1)-C(2) = 129.6(2)^\circ$ . As already stated in [6], this asymmetry is based on steric and electronic factors. Structural parameters within the two rings show further peculiarities in this portion of the molecule; isoxazolone ring bond distances are consistent with extended  $\pi$  delocalization over the  $C(3)-N(1)-O(2)-C(1)-O(2)$  fragment, while slight the differences in double bond lengths for  $C(3)-N(1)$  and  $N(2)-C(4)$  ( $1.280(3) \text{ \AA}$  and  $1.266(3) \text{ \AA}$ , resp.) may be determined by the different H-bonds in which N(1) and N(2) are involved. The pyrrole N-atom N(2), besides a weak intramolecular interaction with H(24) at C(24) ( $C(24) \cdots N(2) = 3.072(3) \text{ \AA}$  with  $C(24)-H(24) \cdots N(2) = 90.9(2)^\circ$ ), is involved in a strong H-bond with the crystallization solvent MeOH ( $O(3) \cdots N(2) = 2.910(3) \text{ \AA}$  with  $O(3)-H(3) \cdots N(2) = 163.2(1)^\circ$ ). Further weak intermolecular H-bonds involve all the O-atoms. The H-bonds, together with the normal *Van der Waals* interactions, are responsible for the unusual crystalline packing. Selected geometrical parameters together with solid-state X-ray data are reported in *Table 1*. Experimental data are in good agreement with *ab initio* calculations. The differences affecting the Ph and Me groups are due to the low-level basis set employed, while the differences in bond lengths relative to the heteroatoms are essentially due to the H-bonds present in the crystalline state. *Ab initio* calculations were good predictors of the great asymmetry in the bond angles around the carbonyl group. As expected, because of the conforma-

Table 1. Selected Bond Lengths [ $\text{\AA}$ ], Bond Angles, and Torsion Angles [ $^\circ$ ] for Compound **3** (by X-ray-diffraction determination [RX] and by computation [HF])

	RX	HF/6-31G(d):3-21G(d):AM1
C(2)–C(3)	1.501(2)	1.509
C(2)–C(1)	1.513(3)	1.521
C(2)–C(4)	1.536(3)	1.541
C(2)–C(6)	1.563(3)	1.558
C(1)–O(1)	1.194(2)	1.179
C(1)–O(2)	1.359(2)	1.341
O(2)–N(1)	1.447(2)	1.382
N(1)–C(3)	1.280(2)	1.269
C(3)–C(7)	1.472(3)	1.457
C(6)–C(13)	1.519(2)	1.470
C(6)–C(5)	1.548(2)	1.561
C(5)–N(2)	1.481(2)	1.473
C(5)–C(19)	1.511(3)	1.481
N(2)–C(4)	1.266(2)	1.249
C(4)–C(25)	1.492(3)	1.519
C(3)–C(2)–C(4)	118.21(15)	117.22
C(1)–C(2)–C(4)	110.10(15)	108.56
C(3)–C(2)–C(6)	114.77(15)	116.46
C(1)–C(2)–C(6)	113.36(15)	116.86
O(1)–C(1)–O(2)	121.88(19)	123.00
O(1)–C(1)–C(2)	129.62(19)	129.14
O(2)–C(1)–C(2)	108.50(16)	107.79
C(1)–O(2)–N(1)	109.66(14)	111.49
C(3)–N(1)–O(2)	108.39(15)	109.34
C(4)–N(2)–C(5)	110.73(16)	110.77
N(1)–C(3)–C(7)–C(12)	31.2(3)	30.74
C(2)–C(6)–C(13)–C(14)	–73.0(2)	–73.67
N(2)–C(5)–C(19)–C(24)	57.5(2)	53.46

tional rigidity, the torsion angles calculated are also very similar to the corresponding experimental values.

The molecule **4** (Fig. 2) is constituted of an *N*-unsubstituted pyrrole ring: a Me group is bonded to C(1) ( $C(1)–C(7) = 1.488(3) \text{ \AA}$ ) and a *O*-(benzamidoxy)carbonyl to C(2), while C(3) and C(4) bear Ph groups. The bond distances and the planar arrangement (maximum deviation from the least-squares plane is  $0.006(2) \text{ \AA}$  for C(1)) confirm the aromaticity of the pyrrole ring. Bond distances and angles ( $C(1)–C(2) = 1.390(3) \text{ \AA}$ ;  $C(2)–C(3) = 1.436(3) \text{ \AA}$ ;  $C(3)–C(4) = 1.361(3) \text{ \AA}$ ;  $C(1)–N(1)–C(4) = 111.3(2)^\circ$ ) are in good agreement with the corresponding values reported for 2,5-dimethyl-4-(2-(phenylmethyl)benzoyl)-1*H*-pyrrole-3-carboxylate [7]. Between the bonds  $C(1)–N(1)$  and  $C(4)–N(1)$  ( $1.351(3)$  and  $1.388(3) \text{ \AA}$ , resp.), the shorter bond is affected by the electroic effect of the Me C-atom C(7), which is co-planar with the pyrrole ring (maximum deviation  $0.002(2) \text{ \AA}$ ). Steric requirements force the Ph rings at C(3) and C(4) to rotate with respect to the pyrrole ring by  $69.13(9)^\circ$  and  $38.2(1)^\circ$ , respectively, and by  $72.42(9)^\circ$  with respect to each other, thus minimizing reciprocal steric interactions and interactions with the carbonyl O-atom O(2) ( $C(8) \cdots O(2) 2.837(3) \text{ \AA}$ ). The C–CO–O group is slightly rotated with respect to the five-

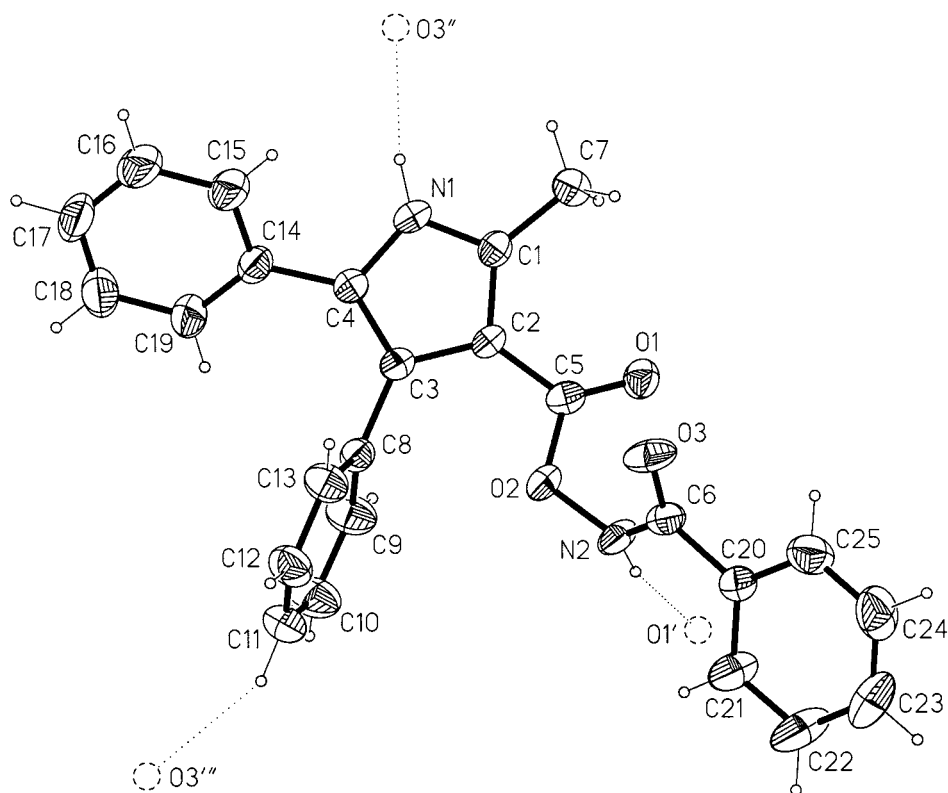


Fig. 2. Molecular drawing of compound 4 showing the atom numbering scheme. Thermal ellipsoids are at 40% of probability and H size is arbitrary. Dotted lines represent the intermolecular H-interactions [(<sup>(1)</sup>)  $1-x, -y, -z$ ; (<sup>(2)</sup>)  $-x, -y, -z$ ; (<sup>(3)</sup>)  $x, -y-1/2, z+1/2$ ].

membered ring, as can be seen from the C(1)–C(2)–C(5)–O(1) ( $-16.1(4)^\circ$ ) torsion angle. While C–CO–O bond distances are typical of this fragment, and the large O(1)–C(5)–C(2) bond angle ( $128.5(2)^\circ$ ) is mainly determined by steric hindrance between O(1) and the Me group (O(1)⋯C(7) =  $3.035(3)$  Å). The amide group C(6)–O(3)–N(2) is rotated by  $77.73(9)^\circ$  with respect to the C–CO–O and by  $29.2(1)^\circ$  with respect to the Ph ring to which it is directly bonded. The bond distances and angles of the fragment are similar to those found in N,O-dibenzoyl-*N*-(*o*-tolyl)hydroxylamine [8] where, surprisingly, the O(1)⋯O(3) distance is the same ( $3.110(3)$  Å). Few compounds with similar benzoylhydroxylamine groups have so far been structurally characterized [9]. The conformation observed in the solid state has the two-fold purpose of minimizing steric-type effects and favoring intermolecular H-interactions and the only possible intramolecular interaction O(1)⋯H(7c)–C(7). The most important H-bonds, which stabilize the whole crystal packing, are those involving the pyrrole NH H-atoms N(1): N(1)⋯O(3'') =  $2.868(3)$  Å with N(1)–H(1)⋯O(3'')  $168(2)^\circ$  and N(2)⋯O(1') =  $2.880(3)$  Å with N(2)–H(2)⋯O(1')  $166(2)^\circ$ . The

Table 2. Selected Bond Lengths [ $\text{\AA}$ ], Bond Angles, and Torsion Angles [ $^\circ$ ] for Compound **4** (by X-ray diffraction determination [RX] and by computation [HF])

	RX	HF/6-31G(d):3-21G(d):AM1
N(1)–C(1)	1.351(3)	1.341
N(1)–C(4)	1.388(3)	1.386
C(1)–C(2)	1.389(3)	1.376
C(1)–C(7)	1.488(3)	1.503
C(2)–C(3)	1.435(3)	1.443
C(2)–C(5)	1.440(3)	1.463
C(3)–C(4)	1.360(3)	1.360
C(3)–C(8)	1.488(3)	1.446
C(4)–C(14)	1.466(3)	1.447
C(5)–O(1)	1.204(3)	1.193
C(5)–O(2)	1.391(3)	1.351
O(2)–N(2)	1.397(2)	1.378
N(2)–C(6)	1.355(3)	1.396
C(6)–O(3)	1.213(3)	1.190
C(6)–C(20)	1.489(3)	1.479
N(1)–C(1)–C(7)	121.7(2)	121.2
C(2)–C(1)–C(7)	131.8(2)	131.4
C(1)–C(2)–C(5)	121.9(2)	123.3
C(3)–C(2)–C(5)	129.9(2)	129.4
O(1)–C(5)–O(2)	121.6(2)	121.2
O(1)–C(5)–C(2)	128.5(2)	126.7
O(2)–C(5)–C(2)	109.9(2)	112.1
C(5)–O(2)–N(2)	114.2(2)	115.7
C(6)–N(2)–O(2)	117.1(2)	117.7
O(3)–C(6)–N(2)	122.8(3)	119.2
O(3)–C(6)–C(20)	123.3(3)	121.6
N(2)–C(6)–C(20)	114.0(2)	119.2
C(1)–C(2)–C(5)–O(1)	–16.1(4)	–8.8
C(2)–C(5)–O(2)–N(2)	–169.7(2)	178.0
C(5)–O(2)–N(2)–C(6)	75.0(3)	78.3
O(2)–N(2)–C(6)–C(20)	175.1(2)	24.0
C(4)–C(3)–C(8)–C(13)	–68.5(3)	–86.1
N(1)–C(4)–C(14)–C(15)	–37.1(4)	–41.2
N(2)–C(6)–C(20)–C(21)	–30.3(4)	31.6

latter involves inversion-centre-related molecule pairs ( $R_2^2(10)$ ) through the N(2)H–CO(1) group [10].

The conformational structure observed in the solid state is very close to one of the numerous minima in the potential-energy surface. The bond distances and angles calculated are in good agreement with the solid state X-ray-structural parameters; selected bond distances, angles, and some relevant torsion angles are reported in Table 2. The observed differences in bond lengths and angles are generally due to the low-level basis set and, in the case of heteroatoms, are mainly determined by molecular packing and intermolecular H-bonds. Torsion angles, as expected, are somewhat different because of the numerous degrees of conformational freedom present in the molecule.

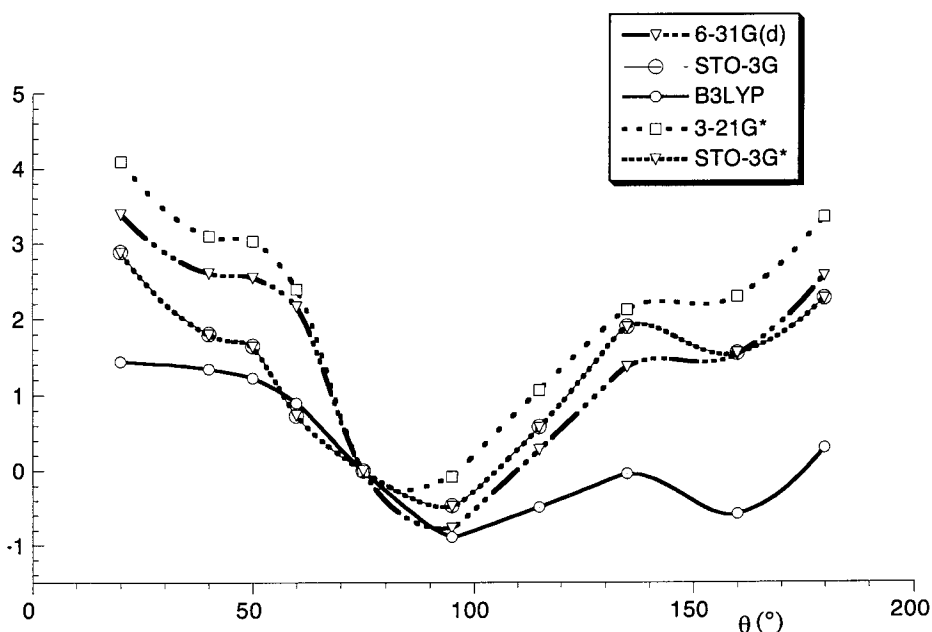


Fig. 3. Variation of torsional potential energy with rotational angle  $\theta$  (C(6)–N(2)–O(2)–C(5)) for compound **4** at the HF/STO-3G, STO-3G\*, 3-21G\*, 6-31G(d), and B3LYP(6-31G(d)) levels

Fig. 3 shows torsional barrier variation around the N–O bond obtained from HF and B3LYP calculations. As can be seen from the picture, both *ab initio* and DFT calculations are able to locate the other two minima near  $90^\circ$  and  $160^\circ$ . Between the conformations observed in the solid state, where a strong intermolecular H-bond is present, and the minimum conformation (at  $\theta \approx 90^\circ$ ), reached at the four levels of calculation, we observe that the molecule is able to form a weak intramolecular H-bond involving O(1) and H(2) ( $\text{H}(2) \cdots \text{O}(1) = 2.58 \text{ \AA}$ ). This H-bond interaction also determines the partial minimum observed at  $\theta = 160^\circ$ , corresponding to  $\text{H}(2) \cdots \text{O}(1) = 2.228 \text{ \AA}$ . Here, however, although the H-bonding interaction is stronger than that mentioned above, the repulsive interaction between the carbonyl O(3) atom and the electronic  $\pi$  cloud of the Ph ring at C(3) ( $\text{O}(3) \cdots (\text{phenyl centroid}) = 3.50 \text{ \AA}$  starts to become significant). The rotational barrier appears to be very low:  $2.33 \text{ kcal mol}^{-1}$  and  $4.16 \text{ kcal mol}^{-1}$  are the maximum and minimum values calculated at B3LYP/6-31G(d) and HF/6-31G(d) levels, respectively. Such torsional barrier energy values are evidence of the great conformational flexibility of the molecule and represent a useful first step in relating structural features to biological properties.

#### Experimental Part

Compound **4** and its precursor **3** were synthesized by modification of the one-pot procedure described in [3]. The intermediate **3** was isolated with an increase in yield (from 10 to 68%) by performing the reaction with an equimolar amount of 3-phenyl-4-benzylideneisoxazol-5(4H)-one (**1**) and 4-methyl-2-phenyloxazol-5(4H)-one (MPO; **2**) [11] in anh. toluene under dry  $\text{N}_2$  and refluxing the mixture for 10 min. The solvent was removed

Table 3. Crystal Data and Structure Refinement for Compounds **3** and **4**

Compound	<b>3</b>	<b>4</b>
Empirical formula	C <sub>26</sub> H <sub>24</sub> N <sub>2</sub> O <sub>3</sub>	C <sub>25</sub> H <sub>20</sub> N <sub>2</sub> O <sub>3</sub>
Formula weight	412.47	396.43
Crystal system, Space group	Triclinic, $P\bar{1}$	Monoclinic, $P2_1/c$
Unit-cell dimensions $a$ [Å]	8.143(1)	10.299(1)
$b$ [Å]	11.053(2)	18.351(3)
$c$ [Å]	12.733(2)	11.626(2)
$\alpha$ [°]	96.89(1)	90
$\beta$ [°]	93.97(1)	108.20(1)
$\gamma$ [°]	105.84(1)	90
Volume [Å <sup>3</sup> ]	1088.3(3)	2087.4(5)
$Z$	2	4
Density (calc.) [Mg/mm <sup>3</sup> ]	1.259	1.261
Absorption coefficient [mm <sup>-1</sup> ]	0.083	0.084
$F(000)$	436	832
Theta range for data collection [°]	1.94–25.05	2.15–25.05
Reflections collected	4249	3978
Independent reflections	3859 ( $R(\text{int}) = 0.0180$ )	3692 ( $R(\text{int}) = 0.0145$ )
Data/restraints/parameters	3859/0/281	3692/0/280
Goodness-of-fit on $F^2$	0.688	0.672
Final $R$ indices ( $I > 2\sigma(I)$ )	$R1 = 0.0392$ , $wR2 = 0.0889$	$R1 = 0.0409$ , $wR2 = 0.0812$
$R$ indices (all data)	$R1 = 0.0857$ , $wR2 = 0.0986$	$R1 = 0.1153$ , $wR2 = 0.0927$
Extinction coefficient	0.023(2)	0.0054(6)
Largest diff. peak and hole [eÅ <sup>-3</sup> ]	0.158 and $-0.246$	0.139 and $-0.132$

under reduced pressure, and the residue was purified by column chromatography (silica gel; CHCl<sub>3</sub>). Subsequently, the treatment of **3** in dioxane/PhCNO 1:2 led to the formation of **4** in almost quant. yield. The physical and spectral data of **3** and **4** are the same as those reported in [3]. A short summary of their X-ray structure determination data is reported in Table 3<sup>3</sup>).

Monocrystals of **3** and **4** suitable for X-ray-analysis were obtained from a MeOH soln. by slow evaporation. Two colorless irregular crystal samples were mounted on the Siemens automated four-circle single-crystal diffractometer *P4*. The diffraction data [12] were collected at room temperature with graphite-monochromated MoK $\alpha$  radiation ( $\lambda = 0.71073$  Å). Lattice parameters for both **3** and **4** were obtained from least-squares refinement of the setting angles of 36 reflections with  $13 \leq 2\theta \leq 28^\circ$ . Suitable correction was needed to allow for the significant crystal decay of **3**, as evidenced by the 43% decrease in intensity in the check reflections monitored of the each 197 measurements. Reflection intensities were evaluated by the profile fitting of a 96-step peak scan among  $2\theta$  shells procedure [13] and then corrected for Lorentz polarization effects. Standard deviations  $\sigma(I)$  were estimated from counting statistics. No of absorption effects were taken into account. The statistics  $|E^2 - 1|$  and systematic absences pointed to the centrosymmetric space groups  $P\bar{1}$  and  $P2_1/c$  for compound **3** and **4**, resp. Data-reduction was performed with the SHELXTL package [14]. Both structures were solved by a combination of standard direct methods [15] and Fourier synthesis, and refined by minimizing the function  $\Sigma w(F_o^2 - F_c^2)^2$  with the full-matrix least-square technique based on all independent  $F^2$  data, with SHELXL97 [16]. All non-H-atoms were refined anisotropically. H-Atoms were included in both the refinements of the 'riding model' method with the X–H bond geometry depending on the parent atom X, while the isotropic displacement parameter was fixed to a single common unrefined value (0.070 and 0.080 Å<sup>2</sup>, resp.). In the model of compound **4**, the two N-bonded H-atoms H(1) and H(2) were located on the difference

<sup>3</sup>) Crystallographic data (excluding structure factors) for the structures reported in this paper have been deposited with the Cambridge Crystallographic Data Centre (CCDC) as supplementary publication No. CCDC-167756 and -167757 for compound **3** and **4**, respectively. Copies of the data can be obtained, free of charge, on application to CCDC, 12 Union Road, Cambridge CB21EZ, UK (fax: +44(1223) 336-033; e-mail: deposit@ccdc.cam.ac.uk).



*Fourier* map and refined as normal isotropic atoms without any constraint. An empirical extinction parameter was included in the final refinement cycles of both models. Both least-difference *Fourier* maps showed no significant electron-density residuals. Final geometrical calculations and drawings were carried out with the PARST program [17] and the Siemens package XP utility, resp. All calculations were performed on a  $\mu$ -VAX 3400 and on a DEC-alpha 3000/400.

*Ab initio* and DFT calculations, molecular modelling, and geometry optimization were carried out on compounds **3** and **4** and on model systems by means of the GAUSSIAN 98 [18] series of programs. *Ab initio* geometry optimization on compound **3** was performed with the keyword ONIOM [19] to divide the molecule into three layers: the central spiro fragment was optimized at HF/6-31G(d) level, while the Me and Ph groups were optimized at HF/STO-3G(d) and AM1 levels, resp. Because of the large computational costs, the geometry of compound **4** was also optimized at three levels using the keyword ONIOM: HF/6-31G(d), HF/3-21G(d), and AM1, for the central fragment, the Me group and the three Ph groups respectively. The conformation of compound **4** obtained from X-ray-analysis with a C(6)–N(2)–O(2)–C(5) torsion angle  $\theta = 75.0(3)^\circ$  was taken as the origin, and its energy set to zero. Internal rotation was studied by scanning the torsion angle ( $\theta$ ) by 10 values from  $20^\circ$  to  $180^\circ$ . For each  $\theta$ , a single-point energy calculation was performed without geometry optimization. Calculations were undertaken at restricted *Hartree-Fock* (RHF) level with STO-3G, STO-3G(d), 3-21G(d), and 6-31G(d), and at density functional theory (DFT) level with Becke's three-parameter hybrid method (B3LYP) and 6-31G(d) [20] as the basis set.

## REFERENCES

- [1] J. C. Powers, J. W. Harper, in 'Protease Inhibitors', Eds. A. J. Barret, G. Salvesan, Elsevier, New York, 1986, 219.
- [2] T. Emery, *Met. Ions Biol. Syst.* **1978**, 7, 77; D. J. Weatherall, in 'Development of Iron Chelators for Clinical Use', Eds. A. E. Martell, W. F. Anderson, D. G. Bosman, Elsevier, North-Holland, New York, 1981, p. 3; K. N. Raymond, M. J. Muller, B. F. Matzanke, *Top. Curr. Chem.* **1984**, 123, 4958; B. H. Lee, M. J. Miller, *Med. Chem.* **1985**, 28, 323; V. Karunaratne, H. R. Hoveyda, C. Orving, *Tetrahedron Lett.* **1992**, 33, 1827.
- [3] G. Grassi, F. Risitano, F. Foti, M. Cordaro, *Synlett* **2001**, 812.
- [4] D. Cremer, J. A. Pople, *J. Am. Chem. Soc.* **1975**, 97, 1354.
- [5] G. A. Molander, C. Kenny, *J. Org. Chem.* **1991**, 56, 1439.
- [6] F. Risitano, G. Grassi, G. Bruno, F. Nicolò, *Liebigs Ann. Chem.* **1997**, 441.
- [7] A. J. Baxter, F. Ince, C. M. Manners, S. J. Teague, *J. Med. Chem.* **1993**, 36, 2739.
- [8] F. Baert, J. Lamiot, D. Couturier, D. Roussel, G. Ricart, *Acta Crystallogr., Sect. C* **1984**, 40, 1071.
- [9] S. Gottlicher, P. Ochsenreiter, *Chem. Ber.* **1974**, 107, 398.
- [10] J. Bernstein, R. E. Davis, L. Shimoni, N. L. Chang, *Angew. Chem., Int. Ed.* **1995**, 34, 1555.
- [11] H. Gotthardt, R. Huisgen, H. O. Bayer, *J. Am. Chem. Soc.* **1970**, 92, 4340.
- [12] Siemens, P3/V, Vax-VMS Version 4.21, Siemens Analytical X-Ray Instruments Inc., Madison, Wisconsin, 1989.
- [13] R. Diamond, *Acta Crystallogr., Sect. A* **1969**, 25, 43.
- [14] G. M. Sheldrick, SHELXTL, VMS Version 5.05, Siemens Analytical X-Ray Instruments Inc., Madison, Wisconsin, 1991.
- [15] A. Altomare, O. Cascarano, C. Giacovazzo, A. Guagliardi, M. C. Burla, G. Polidori, M. Camalli, *J. Appl. Crystallogr.* **1994**, 27, 435.
- [16] G. M. Sheldrick, 'SHELXL97, Program for Crystal Structure Refinement', University of Göttingen, Germany, 1997.
- [17] M. Nardelli, *J. Appl. Chem.* **1995**, 28, 659 (version locally modified).
- [18] M. J. Frisch, G. W. Trucks, H. B. Schlegel, G. E. Scuseria, M. A. Robb, J. R. Cheeseman, V. G. Zakrzewski, J. A. Montgomery Jr., R. E. Stratmann, J. C. Burant, S. Dapprich, J. M. Millam, A. D. Daniels, K. N. Kudin, M. C. Strain, O. Farkas, J. Tomasi, V. Barone, M. Cossi, R. Cammi, B. Mennucci, C. Pomelli, C. Adamo, S. Clifford, J. Ochterski, G. A. Petersson, P. Y. Ayala, Q. Cui, K. Morokuma, D. K. Malick, A. D. Rabuck, K. Raghavachari, J. B. Foresman, J. Cioslowski, J. V. Ortiz, A. G. Baboul, B. B. Stefanov, G. Liu, A. Liashenko, P. Piskorz, I. Komaromi, R. Gomperts, R. L. Martin, D. J. Fox, T. Keith, M. A. Al-Laham, C. Y. Peng, A. Nanayakkara, M. Challacombe, P. M. W. Gill, B. Johnson, W. Chen, M. W. Wong, J. L. Andres, C. Gonzalez, M. Head-Gordon, E. S. Replogle, J. A. Pople, Gaussian 98, Revision A.9, Gaussian, Inc., Pittsburgh PA, 1998.

- [19] M. Svensson, S. Humbel, R. D. J. Froese, T. Matsubara, S. Sieber, K. Morokuma, *J. Phys. Chem.* **1996**, *100*, 19357.
- [20] C. Lee, W. Yang, R. G. Parr, *Phys. Rev. B* **1988**, *37*, 785; A. D. Becke, *Phys. Rev. A* **1988**, *38*, 3098; A. D. Becke, *J. Chem. Phys.* **1993**, *98*, 5648.

*Received July 30, 2001*